Photophysical Investigation of Starburst Dendrimers and Their Interactions with Anionic and Cationic Surfactants

Gabriella Caminati,[†,‡] Nicholas J. Turro,*[,‡] and Donald A. Tomalia*[,§]

Contribution from the Department of Chemistry, Columbia University, New York, New York 10027, and Michigan Molecular Institute, 1910 West St. Andrews Road, Midland, Michigan 48674. *Received March 23, 1990*

Abstract: Fluorescence spectroscopy has been used to characterize the structure of a unique class of anionic macromolecules: starburst dendrimers (SBDs) possessing an external anionic surface. Pyrene was used as a photoluminescence probe to sense various hydrophobic sites in the microheterogeneous architecture offered by poly(amidoamine) starburst dendrimers possessing sodium carboxylated surfaces. A series of 10 different "half-generations, *n*.5" starburst dendrimers, which differ systematically in molecular weight, size, and surface charge density, have been studied. The probe method provides experimental evidence for a structural surface transition between generations 3.5 and 4.5. The same probe method was applied to study how the structural properties of the starburst dendrimers determine their interactions with small ionic amphiphilic molecules. Whereas starburst dendrimers do not noticeably affect the micellization process of an anionic surfactant (sodium dodecyl sulfate, SDS), the association process with a cationic surfactant (dodecyltetrammonium bromide, DTAB) leads to the formation of two different types of SBD-templated surfactant aggregates. Addition of DTAB to aqueous solutions containing the earlier generation (0.5–3.5) SBD leads to the formation of SBD-templated surfactant aggregates that result from noncooperative, random condensation of surfactant molecules on the anionic dendrimer surface. Addition of DTAB to aqueous solutions containing later generation (4.5–9.5) SBDs leads to the formation of SBD-templated surfactant aggregates resulting from initial, noncooperative, random condensation, followed by cooperative condensation of surfactant molecules on the anionic dendrimer surface. The results are shown to be consistent with a change in the morphology of SBDs from an open, branched structure for generations 0.5–3.5 to a closed, increasingly compact surface for generations 4.5–9.5.

Introduction

Starburst dendrimers are a novel class of macromolecules constructed from various initiator cores, upon which radially branched layers, termed generations, are covalently attached.[1a-c] The final exterior layer may be modified chemically to provide a variety of terminal functionalities on the external surface of the dendrimers (see Figure 1 for a schematic description). Starburst poly(amidoamines) (PAMAMs) were the first class of starburst dendrimers to be synthesized and characterized in detail.[1a] The PAMAM dendrimers consist of a nitrogen core (synthesis starting with ammonia, see Figure 2) to which ($=NCH_2CH_2CONHCH_2CH_2N)_2$ repeat units are attached. Throughout the synthesis, the exterior surface may consist of carboxylate groups (termed *n*.5, or half-generations, Figure 1) or of amine groups (termed *n*, or full generations, Figures 1 and 2). Since the dendrimer molecules are covalently bonded and are precisely determined by the method of synthesis, their composition and constitution are well defined.

In contrast to the precise compositional and constitutional aspects of these novel macromolecules, their shapes and morphologies have not yet been defined by direct spectroscopic methods, such as X-ray analysis, due to the fractal nature of their structures, which precludes long-range order. However, molecular simulations[2a] of dendrimer structures have revealed that the dendrimer shape, morphology, and surface structure can be controlled as a function of generation and size. These simulations indicate a rather dramatic change in the dendrimer morphology occurring after the second generation for PAMAM dendrimers (congestion is to be anticipated at some generation from inspection of Figure 1).[2b] For example, the 0-, 1-, and 2-generation dendrimers were found to possess a highly asymmetric shape, whereas the 4 and higher generations are nearly spherical in shape. The 3-generation dendrimer was found to have a transition shape between that of the early and later generations. Furthermore, the early generations were found to possess average structures that were very open, whereas the later generations were more closed, densely packed structures. Thus, since the surfaces of the earlier and later generations are predicted to be structurally quite different, we felt it important to determine the experimental validity of the molecular simulations.

In this report, the fluorescence probe method[3] was used to investigate a series of *n*.5-generation dendrimers possessing anionic surfaces of sodium carboxylate groups (Figure 1). Questions of interest concerning the dendrimer surface, in addition to its morphology, include its binding capabilities, its extent of ionization under various conditions, and its ability to interact with and to organize small molecules. The latter interactions are well-known for the complexes or aggregates formed by the interaction of surfactants with ionic polyelectrolytes such as poly(acrylic acid) or nonionic water-soluble polymers such as poly(ethylene oxide), which have been the subject of a range of investigations in recent years.[4,5] The mechanism of formation of these complexes, their structure, and the nature of polyelectrolyte–surfactant interactions

[†] Permanent address: Dipartimento di Chimica, Università di Firenze, Via G. Capponi 9, 50121 Firenze, Italy.
[‡] Columbia University.
[§] Michigan Molecular Institute.

(1) (a) Tomalia, D. A.; Baker, H.; Dewald, J.; Hall, M.; Kallos, G.; Martin, S.; Roeck, J.; Ryder, J.; Smith, P. *Polym. J. (Tokyo)* **1985**, *17*, 117–132. (b) *Macromolecules* **1986**, *19*, 2466–2469. (c) Tomalia, D. A.; Berry, V.; Hall, M.; Hedstrand, D. M. *Macromolecules* **1987**, *20*, 1164–1167. (d) Tomalia, D. A.; Hall, M.; Hedstrand, D. M. *J. Am. Chem. Soc.* **1987**, *109*, 1601–1603. (e) Padias, A. M.; Hall, H. K.; Tomalia, D. A.; McConnell, J. R. *J. Org. Chem.* **1987**, *52*, 5305–5312. (f) Wilson, L. R.; Tomalia, D. A. *Polym. Prepr. Am. Chem. Soc. Div. Polym. Chem.* **1989**, *30*, 115, 116. (g) Padias, A. B.; Hall, H. K.; Tomalia, D. A. *Polym. Prepr. Am. Chem. Soc. Div. Polym. Chem.* **1989**, *30*, 119, 120. (h) Meltzer, A. D.; Tirrell, D. A.; Jones, A. A.; Inglefield, P. T.; Downing, D. M.; Tomalia, D. A. *Polym. Prepr. Am. Chem. Soc. Div. Polym. Chem.* **1989**, *30*, 121, 122. (i) Tomalia, D. A.; Dewald, J. R. U.S. Patent 4 507 466, 1985; U.S. Patent 4 558 120, 1985; U.S. Patent 4 568 737, 1986; U.S. Patent 4 587 329, 1986; U.S. Patent 4 631 337, 1986; U.S. Patent 4 694 064, 1987. (j) Tomalia, D. A.; Naylor, A. M.; Goddard, W. A. *Angew. Chem.* **1990**, *29*, 139.

(2) (a) Naylor, A. M.; Goddard, W. A., III; Kiefer, G. E.; Tomalia, D. A. *J. Am. Chem. Soc.* **1989**, *111*, 2341. (b) The dendrimer generation system used in earlier work (see refs 1a–i) designated the first star-branched species derived from the initiator core as generation 1.0. The present system is preferred wherein that star-branched intermediate is designated generation 0, thus making it consistent with the geometric progression $Z = N_c N_b{}^G$ for the number of terminal groups (see Figure 1).

(3) Kalyanasundaram, K. *Photophysics of Microheterogeneous Systems*; Academic Press: New York, 1988. (b) Thomas, J. K. *The Chemistry of Excitation at Interfaces*; ACS Monograph; American Chemical Society: Washington, DC, 1984.

(4) Goddard, E. *Colloids Surf.* **1986**, *19*, 255; **1986**, *19*, 301.

(5) Robb, I. D. In *Anionic Surfactants: Physical Chemistry of Surfactant Action*; Lucassen-Reynders, E. H., Ed.; Marcel Dekker: New York, 1981, p 109.

0002-7863/90/1512-8515$02.50/0

Table I. Parameters Relevant to the Size and Surface Characteristics of Starburst Dendrimers

gen	MW	diameters			surface gps		surface area[e]
		SEC[a] (*n*.5, Å)	CPK[b] (*n*.0, Å)	simul[c] (*n*.0, Å)	(*n*.5, no.)	sepn[d] (*n*.5, Å)	(*n*.5, Å^2)
0.5	924	27.9	24.0	21.5	6	12.4	407
1.5	2173	36.2	35.5	31.6	12	12.8	343
2.5	4671	48.3	46.4	41.1	24	12.7	306
3.5	9668	66.1	58.4	53.4	48	12.6	285
4.5	19661	87.9	73.0	63.8	96	11.5	253
5.5	39648	103.9	86.4	76.1	192	10.3	177
6.5	79621	126.8	97.6	86.8	384	9.8	132
7.5	159568	147.3	110.5		768	7.7	89
8.5	319461	174.2	123.5		1536	6.3	62
9.5	639247	210.3	136.5		3072		45

[a] Diameters determined by size exclusion chromatography (SEC) in water. [b] Diameters estimated from CPK models for terminated *n*.0 generations without correction for charge, solvation, etc. [c] Values estimated from interpolation of diameters of the (NH_2) terminated *n*.0 generations without correction for charge, solvation, etc. [d] Distance between surface groups in angstroms. Calculated from experimental SEC diameters assuming the theoretical number of surface groups. [e] Surface area per surface group in angstroms squared. Calculated from experimental SEC diameters assuming the theoretical number of surface groups.

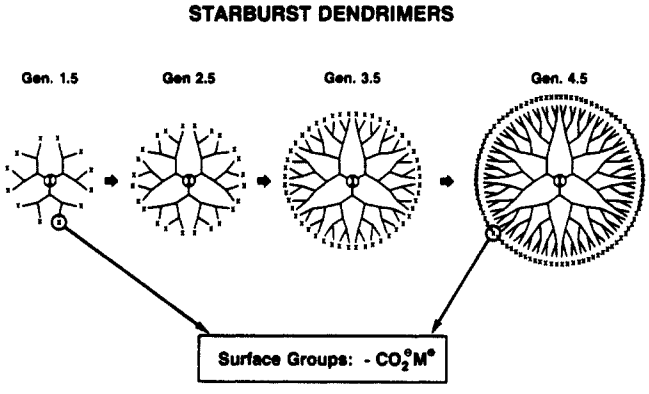

Figure 1. Schematic representation of the structure of typical starburst dendrimers possessing terminal carboxylate groups: generations 1.5–5.5. Note the implied congestion of the surface groups that increases as the generation size increases.

are of interest because of their importance in fields as diverse as enhanced oil recovery, isolation of membrane-bound proteins, polymer solubilization, conformational changes in biopolymers, mineral flotation and flocculation, etc.[6-8] Typically, these studies deal either with aggregates formed between polyelectrolytes and oppositely charged ionic surfactants below the critical micelle concentration (cmc) of the surfactant or with nonionic polymers and micelles of ionic surfactants.[9-11] Recently, Dubin et al.[12] have reported a series of studies on polyelectrolytes above the cmc where precipitation of the polyelectrolyte–micelle complex occurs.

The half-generation (*n*.5) PAMAM dendrimers, as the carboxylate salts (Figure 1), represent a novel family of anionic polyelectrolytes whose structures are reminiscent of micellar aggregates formed from anionic surfactants and polyelectrolytes formed from anionic polymers. In order to obtain information on the structure and behavior of anionic dendrimers and their interactions with ionic surfactants, we have investigated the *n*.5-generation PAMAM family with pyrene as a photoluminescence probe.[3] The structure and dynamics of a wide variety of aggregates and polymers in aqueous environments, such as micelles and polyelectrolytes, have been fruitfully investigated by the use of photoluminescence probes.

Experimental Section

Materials. The synthesis of the starburst dendrimers (SBDs) was described in previous papers.[1] Throughout this paper, sodium salts obtained by the hydrolyses of methyl ester terminated generations with stoichiometric amounts of NaOH in methanol were used (termed the *n*.5-generation SBD; see Figures 1 and 2). Some important physicochemical properties of this family of dendrimers obtained from SEC (hydrodynamic diameters in H_2O) are described in Table I. For comparison, also in Table I are the diameters of the *n*.0 generations determined by appeal to CPK models and to molecular simulation.[2]

Dodecyltrimethylammonium bromide (DTAB) (Sigma) was used as received. Sodium dodecyl sulfate (SDS) (Fischer 99.4%) was recrystallized from methanol. Water was distilled and further purified with a Millipore apparatus. Pyrene (Aldrich 99%) was recrystallized from ethanol.

Methods. Pyrene fluorescence spectra were recorded with a SPEX Fluorolog spectrofluorimeter. All measurements were performed at 293 K with air-saturated samples. The ratio of the intensities of the third to first vibronic peak of fluorescence spectrum of monomer pyrene (I_3/I_1), determined from the experimental spectra, was used as an estimate of the polarity sensed by pyrene microenvironment. Pyrene lifetime measurements were attempted, but the experiments were viciated by the presence of a contribution to the decay due to the starburst dendrimers. Starburst emission intensity in the steady-state measurements was always negligible. All solutions were made with use of pyrene-saturated water (pyrene concentration ca. 4×10^{-7} M) unless otherwise specified.

Results

Aqueous Solutions of SBD and Pyrene. The ratio of vibration-band intensities I_3/I_1 of pyrene fluorescence has been shown to be a faithful reporter[3] of the polarity (hydrophobicity/hydrophilicity) of the pyrene environment. In this study, the pyrene probe is employed to investigate the hydrophobic character throughout a series of 10 generations (i.e., 0.5–9.5-generation SBDs) in the absence and presence of an anionic surfactant and of a cationic surfactant.

The molecular weights of the dendrimers, the diameters of the dendrimers (i.e., for Z = $-CO_2^-Na^+$ in H_2O), the number of surface groups, the distance between surface groups, and the surface areas per group for generations 0.5–9.5 are listed in Table I to serve as a frame of reference for the structural parameters of these macromolecules. For comparison, the diameters of the *n*.0 generations, determined by inspection of CPK models and molecular simulations,[2] are also given in Table I.

In line with results of molecular simulations (and with results to be described in following text), it is convenient to classify the SBDs into "earlier" and "later" generations, with the break coming about the 3.5 generation. For example, from Table I it is noted that there is a break in the distance between the surface groups at the 3.5-generation SBD; i.e., the distance between surface groups is roughly constant (ca. 12.4–12.8 Å) for the "earlier" generations (0.5–3.5) and decreases monotonically (from ca. 11.5–6.3 Å) for the "later" generations (4.5–9.5).

The simplest use of the pyrene probe is to monitor I_3/I_1 as a function of SBD generation for a *fixed concentration of surface*

(6) Seki, K.; Tirrel, D. A. *Macromolecules* **1984**, *17*, 1962.
(7) Taber, J. J. *Pure Appl. Chem.* **1980**, *52*, 1323.
(8) *Interfacial Processes: Energy Conversion and Synthesis*; Wrighton, M. J., Ed.; Advances in Chemistry Series 184; American Chemical Society: Washington, DC, 1980.
(9) Saito, S. J. *Colloid Interface Sci.* **1967**, *24*, 227.
(10) Breuer, M. N.; Robb, I. D. *Chem. Ind.* **1972**, *13*, 531.
(11) Nagarayan, R. *Colloids Surf.* **1985**, *13*, 1.
(12) Dubin, P. L.; Davis, D. D. *Macromolecules* **1984**, *17*, 1294.
(13) Jones, M. J. *Colloid Interface Sci.* **1967**, *23*, 36.
(14) Francois, J.; Dayantis, J.; Sabbadin, J. *Eur. Polym. J.* **1985**, *21*, 165.

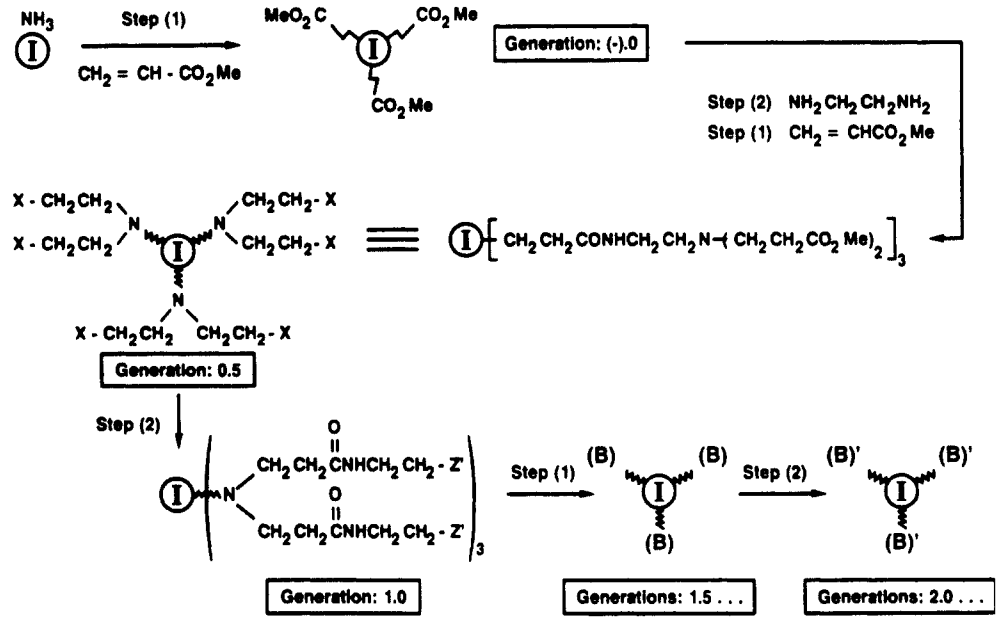

Figure 2. Schematic representation of the synthesis of carboxylate-terminated starburst dendrimers starting from an ammonia core. The *n*.5 ("half") generations are terminated with carboxylate groups (X = CO_2Me), and the full generations are terminated with amino groups (Z = NH_2).

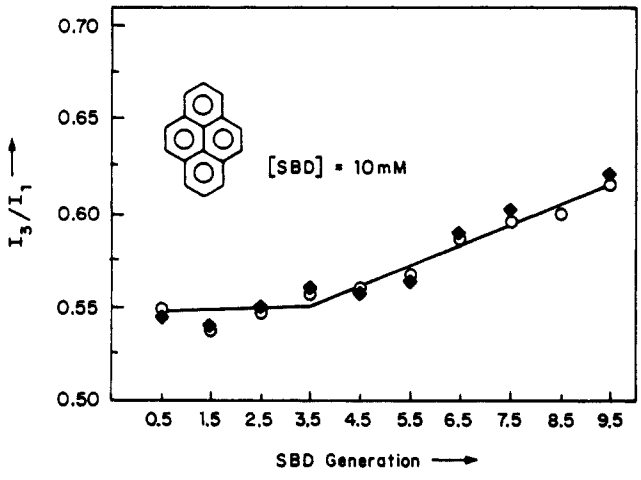

Figure 3. I_3/I_1 ratio of pyrene emission as a function of starburst dendrimer generation: open circles, 10 mM surface groups; closed squares, 5 mM surface groups. The experimental error is 0.003 in the values of I_3/I_1 for duplicate measurements.

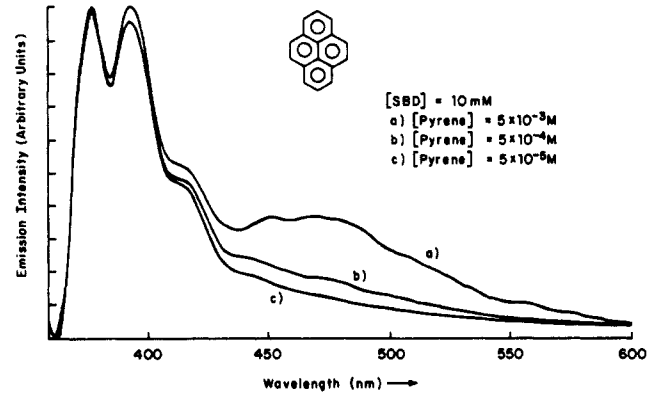

Figure 4. Monomer and excimer emission of pyrene solubilized for the 6.5-generation starburst dendrimer at various concentrations of pyrene. The concentration of pyrene saturated in water is ca. 4×10^{-7} M.

groups. (Throughout this paper, concentrations of SBD refer to the surface (carboxylate) groups, in all cases 10 mM, unless specified.) In this situation, although the absolute number of surface carboxylate groups is constant at 10 mM, the "clustering" of the groups increases as the generation increases and the number of individual starburst molecules decreases (shown schematically in Figure 1).

Typical results are shown in Figure 3 for two concentrations (5 and 10 mM) of SBD in a saturated (ca. 4×10^{-7} M) aqueous solution of pyrene. The value of I_3/I_1 shows little variation with SBD generation for either starburst concentration and remains close to that for pyrene in water for the earlier generations. There is a small and linear increase (which is clearly outside of the experimental error of ca. 1%) in the value of I_3/I_1 for the later generations 4.5–9.5. It should be noted that although the surface-group concentration is the same for all of the generations for samples containing 10 mM SBD, the concentration of SBD *molecules* for 10 mM surface groups varies from 10^{-3} to 2×10^{-6} M in going from generation 0.5 to 9.5.

The variation of I_3/I_1 for the later generations 4.5–9.5 is so small that it might be concluded that the pyrene is not bound at all to the later SBD but that the observed changes in I_3/I_1 are due to changes in the medium induced by the SBD. Evidence for a more intimate interaction between pyrene and the later generation SBDs was available from measurement of the *intensity* of pyrene emission, the *total emission spectrum* of pyrene, and the *solubility* of pyrene in the presence of the later generations.

A significant decrease in the intensity of pyrene emission is observed when later generations of dendrimers were added to saturated aqueous solutions of pyrene. That some of the pyrene is adsorbed on the later generation SBD is further supported by the observation of the enhanced solubility of pyrene in the presence of the later generations (established by UV absorption spectroscopy). Finally, Figure 4 shows the fluorescence spectrum of pyrene observed in the presence of 10 mM 6.5-generation SBD and varying concentrations of pyrene. The excimer emission at 480 nm is apparent and consistent with the adsorption of two or more molecules of pyrene on some SBD. Thus, we conclude that pyrene is adsorbed on the surface of the later generation SBD and that the increase in the value of I_3/I_1 reflects an increase in the hydrophobic sites available to pyrene as the SBD size increases for a fixed number of surface groups.

Aqueous Solutions of SBD, Pyrene, and Sodium Dodecyl Sulfate. The interactions of 1.5- and 6.5-generation SBD with the anionic surfactant, sodium dodecyl sulfate, were examined by the pyrene-probe method, and the results are shown in Figure 5. The observed plots of I_3/I_1 vs [SDS] all possess shapes similar to those for micellar "cmc" curves. The presence of SBD at 10 mM influences the position of the curves slightly, but does not introduce any new features to the shape of the normal cmc curve for SDS.

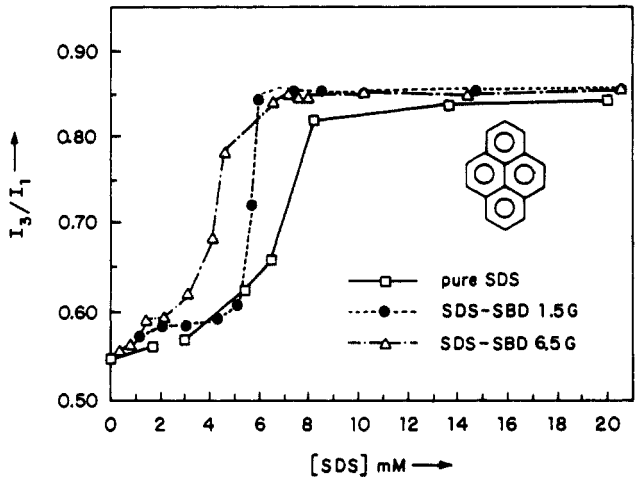

Figure 5. Values of I_3/I_1 for SBD–SDS system as a function of SDS concentration for an "early" (1.5) generation, a late (6.5) generation, and SDS in the absence of SBD.

Thus, the cmc value of 8 mM for SDS in pure water drops to ca. 6 and 4 mM, respectively, when 10 mM 1.5- and 6.5-generation SBDs are present.

The influence of the presence of SBDs on the cmc of SDS is small for all the generations, especially in comparison to the influence of SBDs on the cmc behavior of cationic surfactants to be discussed in the next section.

Aqueous Solutions of SBD, Pyrene, and Dodecyltrimethylammonium Bromide. The interactions of the series of SBDs with a cationic surfactant, dodecyltrimethylammonium bromide, were examined by the pyrene-probe method and are summarized in Figure 6 with representative (1.5-, 3.5-, and 6.5-generation) SBDs. In contrast to the small effect of the presence of SBD on the cmc curves of SDS (Figure 5), there are pronounced effects of SBD on the position of the cmc curves of DTAB relative to that for DTAB alone with all of the generations.

The early generations (0.5–3.5) show curves having the shape of conventional cmc plots (two inflection points, e.g., upper and lower curves of Figure 6), which, however, are displaced with respect to the value of the cmc to lower values as the size of the generation increases. The size of the displacement of the cmc is considerable, however, compared to the situation for SDS. For example, the value of the first inflection point for DTAB in water is at ca. 14 mM, but in the presence of 10 mM 1.5-generation SBD the first inflection point is decreased to ca. 3 mM. It is also noted in Figure 6 that the curve between the inflection points does not rise as sharply in the presence of the 1.5-generation SBD as it does in the case of DTAB in water alone, suggesting less cooperativity in the surfactant interactions. Also, increasing DTAB concentration to a value, C_m (which is slightly above the DTAB cmc), causes the solutions to become milky (presumably because of formation of light scattering colloidal aggregates). The values of I_3/I_1 were found to be stable with time, independent of the sequence of addition of materials, and reversible with respect to the surfactant concentration.

The later generations show curves with a feature that is absent in the curves for the earlier generations: *a second discontinuity appears in the plot*, i.e., two additional inflection points. The plots for the later generations (e.g., 6.5 shown in Figure 6) are reminiscent of those observed for water-soluble polymer/surfactant solutions,[15-17] so we introduce the terminology (Figure 7) and

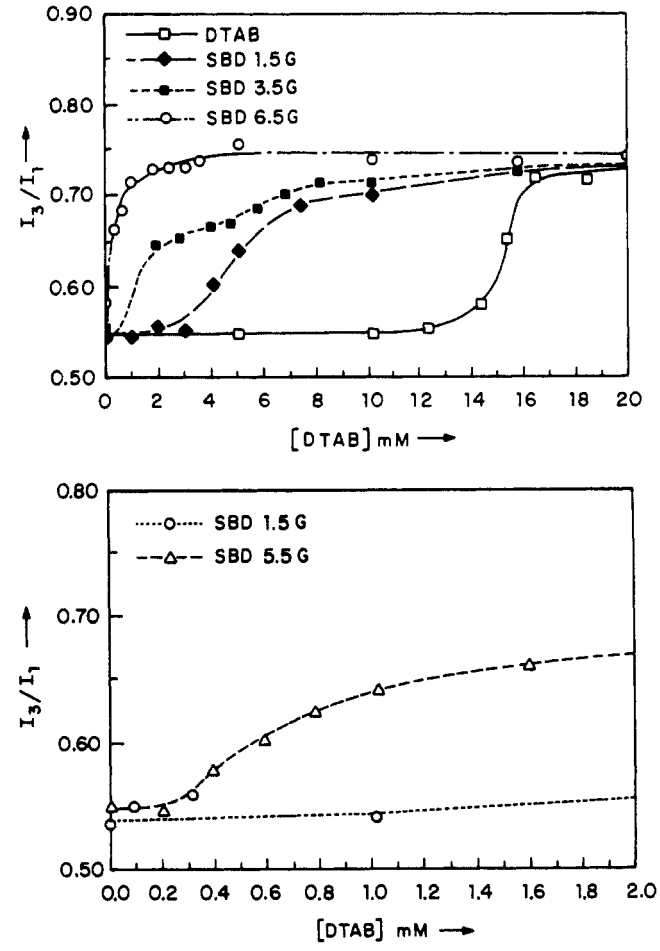

Figure 6. Values of I_3/I_1 for the DTAB–SBD system as a function of DTAB concentration for the 1.5, 3.5, and 6.5 SBD generations (upper curve). The lower curve shows an expanded version of the upper curve for the 1.5 and 6.5 generations, emphasizing the first inflection for the latter generations and its absence in the earlier generations.

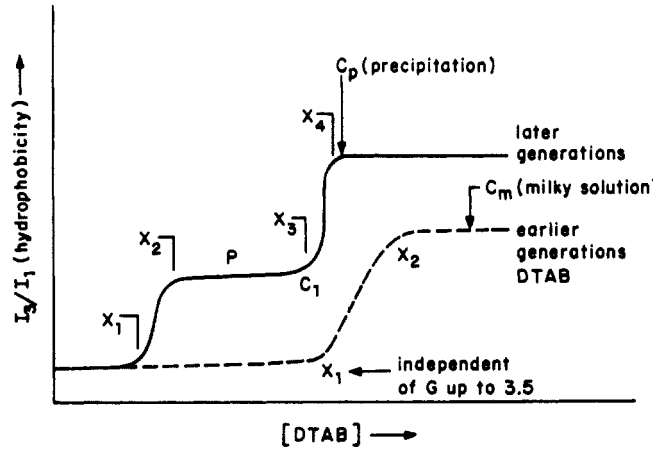

Figure 7. Schematic description of the dependence of I_3/I_1 on the concentration of DTAB in the presence of later generation (upper curve) and earlier generation (lower curve) starburst dendrimers.

concepts employed to describe these systems to serve as a basis for defining, interpreting, and extracting information from the plots of I_3/I_1 vs [DTAB] at fixed concentration of SBD. On the basis of the analogy to polymer/surfactant systems, the first inflection point that occurs at lower surfactant concentration

(15) Dubin, P. L.; The, S. S.; McQuigg, D. W.; Chew, C. H.; Gan, L. M. *Langmuir* **1989**, *5*, 89.
(16) Cabane, B. *J. Phys. Chem.* **1977**, *81*, 1639.
(17) Turro, N. J.; Baretz, B. H.; Kuo, P.-L. *Macromolecules* **1984**, *17*, 231.
(18) Arora, K. S.; Hwang, K.-C.; Turro, N. J. *Macromolecules* **1986**, *19*, 2806.
(19) Turro, N. J.; Kuo, P.-L. *Langmuir* **1987**, *3*, 773.
(20) Turro, N. J.; Gratzel, M.; Braun, A. M. *Angew. Chem., Int. Ed. Engl.* **1980**, *19*, 675.
(21) McGlade, M. J.; Randall, F. J.; Tcheurekdjian, N. *Macromolecules* **1987**, *20*, 1782.
(22) Abuin, E. B.; Scaiano, J. C. *J. Am. Chem. Soc.* **1984**, *106*, 6274.
(23) Zana, R.; Lianos, P.; Lang, J. *J. Phys. Chem.* **1985**, *89*, 41.

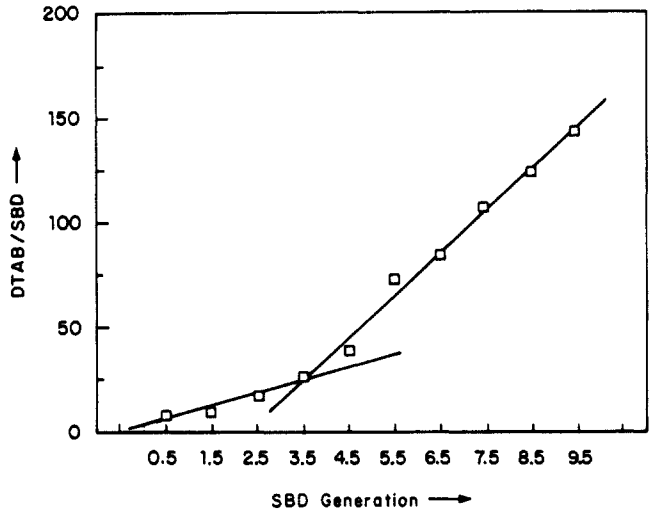

Figure 8. Values of x_2, the concentration of DTAB for the onset of the first plateau region, expressed as the molar ratios of DTAB to SBD surface groups.

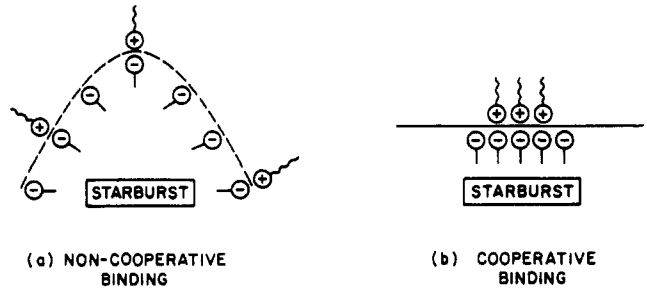

Figure 9. Schematic representation of the (a) primary (random, non-cooperatively bonded aggregates, left) and (b) secondary (cooperatively bonded aggregates, right) formed by adsorption of DTAB surfactant molecules to the anionic surface of a starburst dendrimer.

(termed x_1) is assigned to the onset of condensation of surfactant molecules on the dendrimer surface to form a "primary" aggregate of the dendrimer and surfactant. The concentration x_2 corresponds to the termination of the formation of primary "aggregates". Between x_2 and the third inflection point at concentration x_3, a plateau region occurs in which the number of sites filled by surfactant continues to increase, but the hydrophobicity of the sites remains constant. At x_3 and continuing to x_4, a "secondary" aggregate possessing a higher hydrophobicity begins to form. Beyond x_4 a plateau region again occurs, corresponding to continued condensation of surfactant molecules at available sites on the "secondary aggregates". Often in this region, precipitation (at a concentration C_p) of intermolecular complexes of aggregates is observed. As an example of the magnitude of the influence of higher generation SBDs on the curve displacement, for the 6.5-generation SBD the value of x_2 is less than 1 mM (Figure 6), compared to the value of 14 mM for the DTAB cmc.

For the earlier generations since only one discontinuity is observed, only values of x_1 and x_2 are measurable. For the later generations, which possess two discontinuities, values of x_1, x_2, x_3, and x_4 are measurable.

When the analogy between interactions of water soluble polymers with surfactants and of SBD with surfactants is accepted, the values for x_2 (expressed as the molar ratios of DTAB to SBD) for the series are collected and summarized in Figure 8 and the structures of the primary and secondary aggregates are shown schematically in Figure 9. The values of x_2, which correspond to the onset of the first plateau region, also increase with generation size but possess a break in the rate of increase at the 3.5 generation. These results show that the initial number of surfactants condensing on a SBD depends only on the number of surface groups for the earlier generations, but for later generations, they depend on some other feature of the dendrimer size.

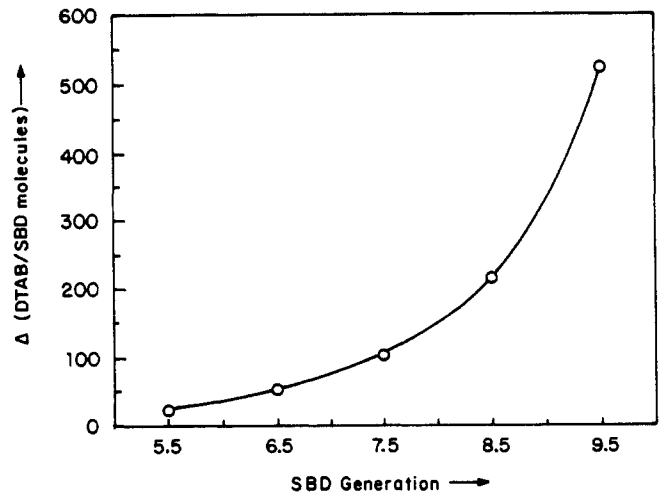

Figure 10. Length of the first plateau (x_2 to x_3) expressed as DTAB molecules to the number of SBD *molecules* as a function of SBD generation.

Table II. Values of x_3 and C_p for High Generations of Starburst Dendrimers

gen	x_3 (DTAB/SBD)	C_p (DTAB/SBD)
4.5	40	56
5.5	96	104
6.5	137	171
7.5	208	350
8.5	340	584
9.5	667	1428

The plateau length, expressed as the difference in the number of DTAB molecules per SBD at the beginning and at the end of the plateau, is plotted in Figure 10 for the later generations (recall that the second plateau is not observed for the earlier generations). As was the case for the values of x_4 and C_p, there is a clear size effect on the plateau length, although it is not linear in the size of the SBD.

For the later generations, the concentration values corresponding to x_3, the end of the first plateau, and to C_p, the onset of a precipitate, are summarized in Table II. From the number of surface groups per generation in Table I it is found that both x_3 and C_p show a *linear correlation with the number of surface groups of the SBD.* Thus, the aggregates that are formed between x_3 and x_4 and that are responsible for the precipitation at C_p depend linearly on the number of surface groups for the later generations.

The limiting value $[(I_3/I_1)_{max}]$, which represents the hydrophobicity of the site sensed by the pyrene probe at x_4, and the values at the first plateau $[(I_3/I_1)_1]$, which represent the hydrophobicity of the site sensed by the pyrene at x_2, provide information complementary to that in Figure 10. The values of $(I_3/I_1)_{max}$ were found to exceed the value obtained for pyrene dissolved in pure DTAB for the later generations, but for the earlier generations the values of $(I_3/I_1)_{max}$ are the same as those for DTAB. Furthermore, the rate of increase of $(I_3/I_1)_{max}$ with the SBD size for the later generations is the same as the rate of increase of the plateau values of I_3/I_1. However, the values of I_3/I_1 are lower than those for pure DTAB until the 7.5-generation SBD is reached.

Influence of Strong Electrolytes. The influence of ionic strength of the interactions between SBD and DTAB was investigated for the 6.5-generation SBD by observing the effect of addition of a strong electrolyte, sodium chloride. The values of I_3/I_1 for 0.1 M sodium chloride as a function of [DTAB] in the presence of 10 mM 6.5 generation were measured and compared to the situation in the absence of salt. The strong electrolyte causes a significant shift in the curve to lower values of [DTAB], but the shape of the curve is not changed; i.e., there are still two discontinuities and four inflection points.

Influence of Surface Charge. In order to determine the effect of surface charge on the interactions of the *nonionic* ester of the

6.5-generation SBD (10 mM) and DTAB, a preliminary investigation was made with the use of the I_3/I_1 probe. In the absence of DTAB, the value of I_3/I_1 of 0.54 indicates that pyrene senses a very hydrophilic environment. Interestingly, pyrene's emission intensity was not decreased by adsorption onto the starburst ester. In the presence of DTAB, no aggregation is observed until a DTAB concentration of 41 mM is reached. The latter is a value much larger than the cmc of pure DTAB (16 mM). A I_3/I_1 limiting value of 0.72, only slightly larger than that for pure micelles, is rapidly reached in the presence of the 6.5-generation starburst ester.

Discussion

Pyrene and Starburst Dendrimer Interactions. The information obtained by the pyrene-probe method is broadly consistent with a model in which the SBDs behave as ordinary electrolytes for the earlier generations (0.5–3.5) and as a novel type of polyelectrolyte or anionic adsorption surface for the later generations (4.5–9.5). This break in behavior coincides with the predicted change in the morphology of the SBD structure and the increasing compactness of the surface groups that are expected to occur around the 3.5 generation, on the basis of molecular simulations.[2] We shall interpret the results with these ideas in mind.

The results of Figure 3 show that pyrene only slightly interacts with the earlier generations remaining in a hydrophilic moiety (values of I_3/I_1 identical with those for pyrene in water). However, that some interactions occur for the later generations is apparent from the systematic increase in I_3/I_1 (pyrene sensing a more hydrophobic environment) as the generation size is increased to 4.5 and beyond. An increase in the UV absorbance beyond the water-saturation value and the observation of excimer formation (Figure 4) in the presence of the later generations is further support for pyrene–SBD interactions. In particular, excimer formation requires at least two pyrene molecules to be located on a single SBD. Nevertheless, the values of I_3/I_1 reflect a *highly hydrophilic binding site for the pyrene that is easily accessible to water, even for the later generations.*

The structural nature of the site of the binding is not revealed by the I_3/I_1 measurements, but there is no reason to believe that the pyrene is adsorbed very far beyond the external carboxylate surface. In analogous anionic micelles (SDS),[3] pyrene is known to bind in the highly polar palisade region of micellar aggregates and should therefore be able to bind to the surface region of the SBD. As the generation of the SBD increases, the surface density and proximity of the surface groups decreases (Table I); i.e., the external shell becomes more densely packed. The increasing values of I_3/I_1 show that this more densely packed surface provides weakly hydrophobic sites for pyrene binding. Recall that the number of sites remains constant (although the degree of ionization of the carboxylate groups will also be changing). The observation of quenching of pyrene emission upon binding to the earlier generation SBD is associated with more intimate interactions of the pyrene excited state with surface carboxylate groups, since control experiments show that pyrene is only weakly quenched by 10 mM and higher concentrations of sodium acetate in water solution. However, the observation that the extent of quenching decreases as the generation size increases is consistent with protection of the pyrene from the ionized carboxylate groups, possibly through siting into the core of a "palisade" layer just beyond the surface layer. The observation that, in the presence of the 6.5-generation completely esterified dendrimer, no quenching of the pyrene emission occurs is further support that the pyrene emission quenching is due to the charged carboxylate groups on the dendrimer surface.

Interactions between Starburst Dendrimers and SDS. The results indicate that the interactions between the anionic surfactant SDS and anionic SBD are weak (Figure 5); i.e., SDS cmc's are only slightly modified by the presence of SBD, and I_3/I_1 vs [SDS] curves maintain the typical cmc shape. Thus, it appears that pyrene interacts preferentially with and is adsorbed on SDS micelles rather than on the SBD in the presence of any of the SBD generations studied. In effect, the pyrene monitors SDS surfactant aggregation processes rather than surfactant–SBD aggregation.

The observed small shift in cmc of SDS in the presence of SBD is attributed to a salt effect. The higher concentration of Na^+ ions in the presence of SBD will screen more efficiently the surfactant head groups and cause a decrease in the cmc. Such an effect depends only on the Na^+ ion concentration, which is kept nearly constant at 10 mM for each generation so that no significant differences are expected among the various generations, as is observed.

Interactions between Starburst Dendrimers and DTAB. The most interesting results obtained in this investigation involve the interactions of the cationic surfactant, DTAB, and the various generations of SBD. In interpreting the results of the probe method for investigating the interactions between SBD and DTAB, it is informative to consider the quantitative parameters of the DTAB micellar structure and the SBD structure and size listed in Table I (especially the abrupt decrease in the distance between carboxylate groups at the 3.5-generation SBD) and to keep in mind the predicted change in morphology[2] from an open to a closed surface around generation 3.5.

The cmc for DTAB is ca. 18 mM, its aggregation number is ca. 50 (and therefore it possesses 50 charged head groups), and its micellar radius is ca. 30 Å. From Table I, the 1.5-generation SBD possesses a diameter of 36 Å and 12 surface groups with an average separation between surface groups of ca. 13 Å. The 6.5-generation SBD possesses a diameter of ca. 130 Å and nearly 400 surface groups with an average separation of ca. 10 Å. Thus, *DTAB micelles are comparable with respect to size and number of surface groups only with the first several members of the earlier generations.*

It is obvious from the results summarized in Figures 6, 7, and 9 that the environment sensed by pyrene at fixed concentration of SBD surface groups (typically 10 mM) and variable concentration of DTAB depends on the starburst generation in a systematic fashion. The first important systematic result is the monotonic general displacement of the entire I_3/I_1 vs [DTAB] curves to lower values of [DTAB] as the generation size increases. The second important systematic result is the appearance of a second inflection point starting with the 4.5 generation and continuing with the remaining higher generation SBD.

The general displacement of the I_3/I_1 vs [DTAB] curves could be due to a simple salt effect, since added electrolytes are well-known to displace micellar cmc curves to lower concentrations of surfactant (as was observed for SDS). However, for the 10 generations investigated, the concentration of surface groups, and therefore the concentration of salt, are held fixed (i.e., at 10 mM). Since the positions of the curves are spread over orders of magnitude of [DTAB], we can reject the possibility that a classical salt effect to induce formation of DTAB micelles is responsible for the discontinuities shown in Figure 6 and that were observed for all of the generations.

A similar structural SBD parameter that appears to correlate with the break in shapes of the I_3/I_1 vs [DTAB] curves at the 3.5-generation SBD is available from Table I: the distance between surface groups or the surface area per surface group. The separations between surface groups for the 0.5–3.5-generation SBDs are all 12.6 ± 0.2 Å, whereas at the 4.5 generation the distance abruptly drops to 11.5 Å and then *linearly* decreases with the starburst generation. *The combination of smaller distance between surface groups and the larger size of the SBD* (there is no break in the diameter as a function of starburst generation) *favors cooperative interactions of the condensed DTAB molecules starting with the 4.5-generation SBD.* The smaller distance is favorable because adjacent surfactants can better enjoy stabilizing hydrophobic interactions resulting from greater intimacy of the surfactant hydrocarbon chains. The larger size may be favorable because the "flattening" of the "curvature" of the surface with increasing size should allow less distortion of the chains as they attempt to maximize stabilization (Figure 9). In addition, for the earlier generations the size of the dendrimer is too small for effective cooperative adsorption of the surfactant.

From these considerations, we suggest the following candidates for the sites that the pyrene probe senses and binds to in solutions

containing SBD and DTAB. The first site (I) is the most hydrophobic region of the external portion of the charged surface of the SBD that is free of surfactant (e.g., regions containing unionized carboxylate groups). The second site (II) is the region of the external portion of the charged surface of the SBD that possesses surfactant molecules that are *noncooperatively and randomly distributed* about the charged external dendrimer surface. The third site (III) is the most hydrophobic region of an aggregate of a SBD and DTAB for which the surfactant molecules are *cooperatively bound* to the dendrimer external surface to form "mixed micellar" clusters on the dendrimer surface. These micellar clusters are expected to be smaller than the micelles of DTAB in water and to have a size and number that depends on the SBD size and on the DTAB concentration. The fourth site (IV) is the most hydrophobic region of intermolecular complexes formed between SBD–DTAB aggregates themselves or with DTAB micelles. Finally, DTAB micelles, whose size is perturbed by the presence of the SBD molecules, are also potential sites (V) for the pyrene probe.

With the above considerations in hand we now interpret the results of the investigation of the interactions of starburst dendrimers with the cationic surfactant DTAB and for the purposes of discussion shall employ Figure 7 as a paradigm that idealizes a plot of I_3/I_1 vs [DTAB] for aqueous systems of a typical earlier and a typical later generation of the SBD and Figure 8 to describe schematically the important structures for binding of pyrene.

The general curve for the earlier generations shows only two inflection points at concentrations x_1 and x_2 and has the appearance of a typical micellar cmc curve. However, for the earlier generations that show only these two inflection points, the rising portion of the curve between x_1 and x_2 is not as steep as it is for the pure surfactant. Furthermore, at the concentration C_m, which occurs substantially beyond x_2, the solutions become milky in appearance. The general curve for the later generations shows four inflection points characterized by concentrations x_1, x_2, x_3, and x_4, and by a plateau region, P, between concentrations x_2 and x_3. In addition, at a concentration C_p, which is slightly higher than x_4, a precipitate is observed to form for all members of the later generations.

Of the five possible sites under consideration, the external charged surface of the SBDs themselves (site I) and DTAB micelles (site V) are ruled out for the major portions of the I_3/I_1 vs [DTAB] profiles. The SBD surfaces are eliminated because the values of I_3/I_1 are much higher (more hydrophobic) than those in the absence of DTAB, even at the lowest concentration of added DTAB. The native DTAB micelles are eliminated because the displacements of the curves at fixed surface concentration depend in a monotonic manner on the starburst generation (even for the earlier generations) and because the displacements are enormous relative to those expected for relatively dilute (10 mM) salt concentration. Therefore, we interpret the result in terms of three sites (II–IV) only; aggregates between SBD and DTAB for which the surfactants are randomly distributed over the surface (termed A_r aggregates), aggregates for which the surfactants are cooperatively associated on the surface (termed A_c aggregates), and intermolecular complexes (of either) of these aggregates with themselves or with DTAB micelles (termed A_i aggregates).

For the earlier generations, our results are consistent with the formation of A_r aggregates of SBD–DTAB at x_1. For these aggregates, the surfactant is randomly bound on the dendrimer surface; in addition, some normal DTAB micelles may be present in ever increasing amounts as the DTAB cmc is approached. Since the binding is expected to be random for the A_r aggregates, the slope of the I_3/I_1 vs [DTAB] is not sharp, the binding of pyrene is relatively weak, and the pyrene senses a very hydrophilic site. At x_2, the formation of DTAB micelles probably competes with the SBD–DTAB aggregates for the site of pyrene binding and the limiting value of I_3/I_3 reaches that expected for DTAB micelles. As the [DTAB] is increased further, at C_m (close to the DTAB cmc) complexes of the A_i type are formed between the SBD–DTAB aggregates and DTAB micelles or A_i type intermolecular complexes of SBD–DTAB aggregates form, either of which will impart a milky appearance to the solutions.

For the later generations, our results are consistent with the portion of the curve between x_1 and x_2 corresponding to the random condensation of the cationic surfactant on the anionic dendrimer by electrostatic interactions to form A_r aggregates of DTAB and SBD; i.e., the surfactant molecules condense noncooperatively and randomly about the dendrimer surface. The plateau region between x_2 and x_3 corresponds to the continued deposition by electrostatic interactions of surfactant onto the A_r aggregates. The portion of the curve between x_3 and x_4 corresponds to the onset of cooperative condensation of surfactant to form A_c aggregates, and the final portion of the curve beyond x_4 corresponds to formation of condensation of the A_c aggregates to form A_i aggregates that precipitate.

The surface of the random A_r aggregates is expected to be more hydrophobic than the SBD surface itself but less hydrophobic than the micellar clusters formed by the A_c aggregates; i.e., the noncooperative binding of the surfactant does not induce the clustering of surfactants that would produce hydrophobic pockets to which the pyrene could be adsorbed. The pyrene adsorbed on the A_r aggregates can associate with one or several surfactant molecules, but not with a significant cluster of surfactant molecules. The structure of the A_c aggregates is postulated to be more hydrophobic than that of the primary aggregates because of cooperative condensation of surfactants to form micellar (or hemimicellar) structures on the dendrimer surface. The structure of the condensed secondary aggregates is postulated to be even more hydrophobic than DTAB micelles because the micellar portions of the A_c aggregates fuse together to form large "mixed micelles" with the SBD.

The data in Figure 8 show that for the earlier generations the number of DTAB molecules that condense on a SBD does not depend as strongly on dendrimer size as it does on the number of surface groups; i.e., [DTAB]/[SBD] is roughly constant for generations 0.5–3.5. This observation is further support for the noncooperative binding of the surfactant to the surface of the earlier generation dendrimers, since cooperative binding would be expected to depend strongly on the dendrimer size. Indeed, the number of DTAB molecules per surface group rapidly increases beyond the 4.5-generation SBD, consistent with the onset of cooperative binding for the later generations.

As mentioned previously, for the later generations the I_3/I_1 vs [DTAB] curves are reminiscent of those for the aggregation of surfactants and water-soluble polymers.[15-17] For example, the observation of two plateaus has been noted for anionic surfactants and water-soluble polymers, and the shape of the "cmc" curves has been ascribed to the formation of "mixed micelles" (smaller than those formed in pure water) surrounded by polymer chains.[17] However, it should be pointed out that this literature report differs from ours in two respects: with linear polymers the first discontinuity point is not many orders of magnitude smaller than the surfactant cmc, as we observe, and the second discontinuity point is at a surfactant concentration that is higher than the cmc, not lower, as we observe. Of course, an important difference between the SBD and conventional surfactant micelles is the dimension of the SBD molecules (Table I) and the high surface charge density, which increases with increasing generation. Furthermore, the distance between the surface groups is relatively small and could enhance hydrophobic interactions between two surfactant molecules adsorbed on proximate sites.

The plateau length (Figure 10) shows a specific dependence on the size of the generation for the later generations. The length of the plateau, expressed as the molecular ratio of DTAB to SBD *molecules*, continuously increases as the SBD size increases. This dependence of the number of surfactant molecules condensed on a SBD on the size of the SBD appears to exclude a purely electrostatic mechanism for aggregation, especially when the results are contrasted with those for the earlier generations that show a negligible dependence of the number of adsorbed DTAB molecules on the SBD size.

From the number of surface groups in Table I and the data in Table II, it is found that a plot of the values of C_m (or C_p) is

linear with the number of surface groups. For each generation, the first plateau ends when one DTAB molecule has added per five SBD surface groups, and precipitation starts when one DTAB molecule has added per two SBD surface groups. Thus, the precipitation phenomena appear to follow a stoichiometry defined by a point at which the surface groups are nearly completely neutralized by association with DTAB molecules. We suggest that the length of the first plateau (Figure 10) correlates with SBD size because the number of micellar clusters that can fit on a starburst surface increases with the size of the surface of an individual SBD molecule; i.e., for the smaller surfaces there is a destabilizing interference between the clusters as they grow.

The observation that the values of I_3/I_1 in the first plateau region increase *linearly* as the starburst generation increases is consistent with increasing hydrophobicity of the micellar aggregates on the dendrimer surface, presumably the result of their increasing size as the dendrimer size increases. Eventually, the value of I_3/I_1 in the plateau region is higher than that of DTAB micelles, reflecting the more strongly hydrophobic environment of the condensed A_c aggregates.

The maximum values of I_3/I_1 do not increase for the earlier generations, but starting with the 6.5-generation SBD the same sensitivity of I_3/I_1 to SBD generation size is found for both the maximum values of I_3/I_1 and the values of I_3/I_1 for the first plateau. This result suggests a similar sensitivity toward hydrophobicity is being monitored in both cases; i.e., cooperatively bound aggregates condensing on the dendrimer surface are involved.

Finally, the general model proposed is consistent with the results obtained in the presence of sodium chloride. Addition of sodium chloride to micellar solutions causes micellar aggregates to grow in size (and become more hydrophobic) as the result of shielding of the charged groups on the micellar surface. It is also easier for the aggregates to form. The addition of sodium chloride causes the I_3/I_1 vs [DTAB] curve to transpose to lower concentrations of DTAB and leads to higher limiting values of I_3/I_1.

Conclusions

The pyrene fluorescence probe reveals a definite structural dependence of starburst dendrimers that is a function of the dendrimer generation. This is consistent with close packing of surface groups and with molecular simulations that predict a change in surface morphology occurring around generations 3.5–4.5. Such behavior allows classification of the dendrimers into earlier and later generations based on differing observed properties.

The *earlier generations* (0.5–3.5) appear to possess a hydrophilic structure with large separations between the surface groups. This structure is revealed by the values of I_3/I_1, which remain very similar to those for pure water, even when pyrene is adsorbed on the dendrimer surface. Addition of an anionic surfactant (SDS) does not lead to significant dendrimer–surfactant complexing, but the cmc for SDS micelle formation is slightly decreased by addition of SBD, probably as the result of a simple salt effect. Addition of a cationic surfactant (DTAB) to earlier generation SBDs results in formation of A_r aggregates that appear to be randomly and noncooperatively bound to the external, charged dendrimer surface, mainly by electrostatic interactions (Figure 9, left). Pyrene senses an environment that is weakly hydrophobic when bound to these aggregates, but as more DTAB is added to the solutions, the bound pyrene is readily displaced to the DTAB micelles that are also formed in the presence of the earlier generations.

The *later generations* of SBD appear to possess a more hydrophobic and congested outer surface, with more closely packed head groups (Figure 9, right). Pyrene bound to these dendrimers is probably bound in the hydrophilic palisade layer of the dendrimer, a small distance from the charged surface groups. An important feature of the closed structure of the later generations is that they assume polymerlike properties and can induce cooperative interactions among bound surfactant molecules. Thus, for the later generations the addition of DTAB first occurs in a noncooperative manner via electrostatic binding, but at higher concentration cooperative binding causes aggregation of surfactant to form micellar structures on the dendrimer surface. This cooperative binding is suggested to result from alkyl chain association that is induced by the closely packed charged groups on the dendrimer surface. At a high enough concentration of DTAB, these aggregates condense to form interpolymeric complexes that precipitate from the solution.

In summary, it appears that the fluorescence probe method can be profitably employed to investigate the structure of starburst dendrimers and their interactions with surfactant molecules in aqueous solution. The results are consistent with a change in morphology between generations 3.5 and 4.5, which leads to a transformation from an open, branched surface structure to a closed, compact surface structure.

Acknowledgment. G.C. and N.J.T. thank the NSF, the AFOSR, and IBM for their generous support of this research. G.C. thanks the Italian M.P.I. (Ministero Publica Istruzione) for financial support. D.A.T. thanks the New Energy and Development Organization (NEDO) of the Ministry of International Trade and Industry of JAPAN (MITI) for generous support of certain critical synthetic efforts.

Registry No. Pyrene, 129-00-0; sodium dodecyl sulfate, 151-21-3; dodecyltrimethylammonium bromide, 1119-94-4.